PLOS ONE

RESEARCH ARTICLE

Infiltration of CD3+ and CD8+ lymphocytes in association with inflammation and survival in pancreatic cancer

Gerik W. Tushoski-Alemán[1], **Kelly M. Herremans**[1], **Patrick W. Underwood**[1], **Ashwin Akki**[2], **Andrea N. Riner**[1], **Jose G. Trevino**[1], **Song Han**[1], **Steven J. Hughes**[1]*

1 Department of Surgery, College of Medicine, University of Florida, Gainesville, Florida, United States of America, 2 Department of Pathology, College of Medicine, University of Florida, Gainesville, United States of America

* Steven.Hughes@surgery.ufl.edu

Abstract

Background

Pancreatic ductal adenocarcinomas (PDAC) have heterogeneous tumor microenvironments relatively devoid of infiltrating immune cells. We aimed to quantitatively assess infiltrating CD3+ and CD8+ lymphocytes in a treatment-naïve patient cohort and assess associations with overall survival and microenvironment inflammatory proteins.

Methods

Tissue microarrays were immunohistochemically stained for CD3+ and CD8+ lymphocytes and quantitatively assessed using QuPath. Levels of inflammation-associated proteins were quantified by multiplexed, enzyme-linked immunosorbent assay panels on matching tumor and tissue samples.

Results

Our findings revealed a significant increase in both CD3+ and CD8+ lymphocytes populations in PDAC compared with non-PDAC tissue, except when comparing CD8+ percentages in PDAC versus intraductal papillary mucinous neoplasms (IPMN) (p = 0.5012). Patients with quantitatively assessed CD3+ low tumors (lower 50%) had shorter survival (median 273 days) compared to CD3+ high tumors (upper 50%) with a median overall survival of 642.5 days (p = 0.2184). Patients with quantitatively assessed CD8+ low tumors had significantly shorter survival (median 240 days) compared to CD8+ high tumors with a median overall survival of 1059 days (p = 0.0003). Of 41 proteins assessed in the inflammation assay, higher levels of IL-1B and IL-2 were significantly associated with decreased CD3+ infiltration (r = -0.3704, p = 0.0187, and r = -0.4275, p = 0.0074, respectively). Higher levels of IL-1B were also significantly associated with decreased CD8+ infiltration (r = -0.4299, p = 0.0045), but not IL-2 (r = -0.0078, p = 0.9616). Principal component analysis of the inflammatory analytes showed diverse inflammatory responses in PDAC.

Conclusion

In this work, we found a marked heterogeneity in infiltrating CD3+ and CD8+ lymphocytes and individual inflammatory responses in PDAC. Future mechanistic studies should explore personalized therapeutic strategies to target the immune and inflammatory components of the tumor microenvironment.

Background

Pancreatic ductal adenocarcinoma (PDAC) exhibits complex molecular and cellular heterogeneity, and clinical outcomes remain poor [1]. Compared to other tumor types, PDAC is considered an immune-cold cancer, escaping immune recognition by cytotoxic T-cells (CD8+), and other anti-tumor immune cell types. It is also resistant to immune checkpoint inhibition monotherapy [2,3]. Complex inflammatory processes have been shown to modulate PDAC progression [4,5]. For example, we and others have demonstrated that cancer associated fibroblasts (CAFs) impact the tumor microenvironment and foster tolerance [6,7]. Although PDAC is typically described as a non-immunogenic tumor, reprogramming the dense desmoplastic reaction, and resulting inflammatory response may offer therapeutic opportunities for patients.

The activation and recruitment of CD3+ and CD8+ lymphocytes are fundamental to mounting an effective tumor response in nearly all cancers. Various techniques have been employed to evaluate lymphocyte populations. Semi-quantitative approaches are routinely applied in clinical and diagnostic settings. Quantitative and automated approaches have been shown to enable standardized analysis of large datasets, enhanced reproducibility, and precision in anticipating immunotherapy response [8–10]. These approaches have not yet been fully assessed or compared in PDAC. Neoadjuvant therapy has been shown to alter the immune microenvironment of pancreatic cancers [11,12], and as such, a treatment naïve cohort may offer enhanced insight to true lymphocyte heterogeneity in PDAC. We hypothesize that a quantitative approach could offer improved accuracy in assessing lymphocyte infiltration for overall survival in pancreatic cancer patients. We further hypothesize that infiltrating T-cells are associated with inflammatory proteins in the tumor microenvironment. We anticipate that associations between infiltrating T-cells and inflammatory proteins in the tumor microenvironment may shed light on the underlying mechanisms of T-cell recruitment and activation to provide potential targets to improve therapeutic efficacy in PDAC.

In this study, we assembled tissue-microarrays (TMAs) of treatment naïve PDAC tumor and non-PDAC controls. We quantitatively determined intratumoral CD3+ and CD8+ lymphocyte populations. The design of this study augments previous studies that have relied on semi-quantitative assessment and included neoadjuvant treated PDAC patients [13]. We performed multiplex analysis on matching tumors to assess relationships between immune cell infiltrations and inflammatory proteins in the tumor microenvironment. We also identified multiple inflammatory factors as indicators of high CD3+ or CD8+ involvement.

Methods

Patient cohort and tissue preparation

All studies were approved by the Institutional Review Board at the University of Florida (IRB201600873) and informed consent was obtained from all patients prior to any tissue collection. Patients were recruited into the study from May 2012 to January 2022. This study was conducted from January 2017 to March 2023. Authors had access to information that could

Table 1. Clinicopathological characteristics of patient cohort.

		PDAC (n = 59)	Benign (n = 37)
Age, mean (SD)		69.93 (9.3)	52.59 (14.8)
Race, n (%)	**White**	57 (96.6)	32 (86.5)
	African American	1 (1.7)	5 (13.5)
	Other	1 (1.7)	0 (0)
Sex, n (%)	**Male**	36 (61.0)	13 (35.0)
	Female	23 (39.0)	24 (65.0)
Pathology, n (%)	**PDAC**	59 (100.0)	NA
	Chronic pancreatitis	NA	20 (54.1)
	Intraductal papillary mucinous neoplasm (IPMN)	NA	6 (16.2)
	Mucinous cystic neoplasm	NA	4 (10.8)
	Cyst	NA	2 (5.4)
	Pancreatic neuroendocrine tumor (PNET)	NA	2 (5.4)
	Pseudopapillary neoplasm	NA	1 (2.7)
	Pancreatic intraepithelial neoplasia	NA	1 (2.7)
	Microcystic serous cystadenoma	NA	1 (2.7)
T Stage, n (%)	**I**	1 (1.7)	NA
	II	2 (3.4)	NA
	III	56 (94.9)	NA
	IV	0 (0)	NA
N Stage, n (%)	**0**	7 (11.9)	NA
	I	51 (86.4)	NA
	II	1 (1.7)	NA
Histologic grade, n (%)	**Well-differentiated**	5 (8.5)	NA
	Moderately differentiated	25 (42.4)	NA
	Moderately-to-poorly differentiated	8 (13.5)	NA
	Poorly differentiated	21 (35.6)	NA
Treatment, n (%)	**No neoadjuvant therapy**	59 (100.0)	NA

identify individual patients after data collection. All tissue samples were obtained from our tissue bank at the University of Florida Department of Surgery. Only patients with pathology confirmed PDAC naïve to neoadjuvant chemotherapy or radiation were included in the cancer group. Tissue was also collected separately from patients with pancreatitis, pancreatic cyst, and intraductal papillary mucinous neoplasm (IPMN) to serve as non-PDAC controls. All surgical specimens were collected by sharp dissection on a back table in the operating room. Pancreatic tissues were also collected from patients with chronic pancreatitis or other benign conditions that should not impact the resected pancreas, i.e., duodenal adenoma. Tissue used in the study was collected from distinct and separate patients with the diseases shown in Table 1. Samples were then transported on ice in Dulbecco's modified Eagle media supplemented with 10% fetal bovine serum (Lonza Group) and 1% antibiotic/antimycotic solution (Corning Inc.) to the lab immediately. Samples were flash frozen within 20 minutes of collection and stored at -80˚C for downstream soluble protein analysis. Separately, matching FFPE blocks were requested from our pathology core for TMA assembly.

Tissue microarray assembly

Tissue was formalin-fixed, and paraffin embedded following resection. Representative formalin fixed paraffin-embedded blocks and tumor areas were selected by a pathologist (A.A) based

on H&E-stained slides. Briefly, a hollow needle was used to remove 2 mm diameter tissue cores from regions of interest. These tissue cores were then inserted into a recipient paraffin block forming the TMA. Assembled TMAs for CD3+ and CD8+ lymphocytes originate from the same tumors and tissue. TMAs were randomly assembled in duplicate and subsequently assessed by a pathologist for quality assurance before subjecting to cutting 4-micron slides for subsequent immunohistochemical analyses.

Assessment of tissue microarray

Presence of CD3+ and CD8+ lymphocytes were evaluated by immunohistochemistry using anti-CD3 and anti-CD8 antibodies (Dako Omnis, Agilent). The project pathologist (A.A.) semi-quantitatively graded each core using traditional scoring methodology (scores ranging from 0–3). Scores between each TMA were calculated and compared to quantitative assessment. Slides of the stained TMAs were scanned using an Aperio Scanscope CS microscope and digital images were acquired for quantitative analysis. Quantification of positively stained cells was performed using the software package QuPath 0.3.2. [8,14] (see https://qupath.github.io/). Cores were only excluded if no analyzable tissue was present, or if PDAC was not confirmed for that core. Image type settings in QuPath were set to Brightfield (H-DAB). Total counted cells and positively stained cells (DAB) for each were tabulated using the positive cell count function in QuPath (analyze -> cell detection -> positive cell detection). Whole tissue cores were selected for analysis. Percentage of positive cells were calculated using positive cells / total cells *100 (%). TMAs were stained and assembled in duplicates, averages between two matching TMAs were used, when available. Quantification and grading were performed in a blinded fashion separate from survival analysis. A total of 99 individual cores in the PDAC group, and 36 non-PDAC cores in the CD3+ TMA were graded and quantitated across duplicates. In the CD8+ TMA, 90 individual PDAC cores and 37 non-PDAC cores were graded and quantitated across duplicates. The minor differences in sample sizes were due to quality-assurance (i.e. exclusion due to core integrity/damage across TMAs).

Soluble protein analysis

At the time of processing, tissue was thawed and weighed. Tissue was sharply divided into small pieces and placed into 2-mL Lysing Matrix D tubes (MP Biomedicals, Santa Ana, California, USA). For every 30mg of tissue, 500 uL of cell lysis buffer (Cell Signaling Technology, Danvers, Massachusetts) with Protease/Phosphatase Inhibitor (Cell Signalling Technology) was added. Samples were then placed on ice for 2 minutes each cycle. Lysates were collected and centrifuges at 13,000 relative centrifugal force for 10 minutes. Supernatants were collected and analyzed for total protein concentration. Homogenates were probed for 41 unique analytes using a commercially available multiplex analysis per the manufactures protocol (catalog no. HCYTMAG-60K-PX41; Millipore Sigma) and as described previously [15]. The multiplex assay was selected for its large inflammatory panel and used as exploratory analysis as previously described [15]. Data were acquired with the MAGPIX System (Luminex Corp) and analyzed using MILLIPLEX Analyst 5.1 (Millipore Sigma). Protein concentrations were normalized to total protein concentrations to yield individual analyte concentrations. Of the 41 analytes, those that provided non-informative data (no detection) were excluded. Samples from the TMA and in the soluble protein analysis were matched and originate from the same patient. These samples were processed separately (i.e., formalin fixation/paraffin embedding for the TMA, and sharp frozen for soluble protein analysis) but represent paired tissue after pathological confirmation.

Survival analysis

Overall survival for our patient cohort was retrospectively obtained. Date of death was obtained through retrospective chart verification to determine survival time from surgical resection. Kaplan-Meier tests were applied, and the patient cohort was evenly split between the lower 50th percentile, and upper 50th percentile for CD3+ and CD8+ cell count percentages. Overall survival was also evaluated with semi-quantitative grading, categorizing the groups based on their grade (0, 1, 2, 3). Mantel-Cox survival comparisons were also made between quantification and grading for CD3+ and CD8+ patients.
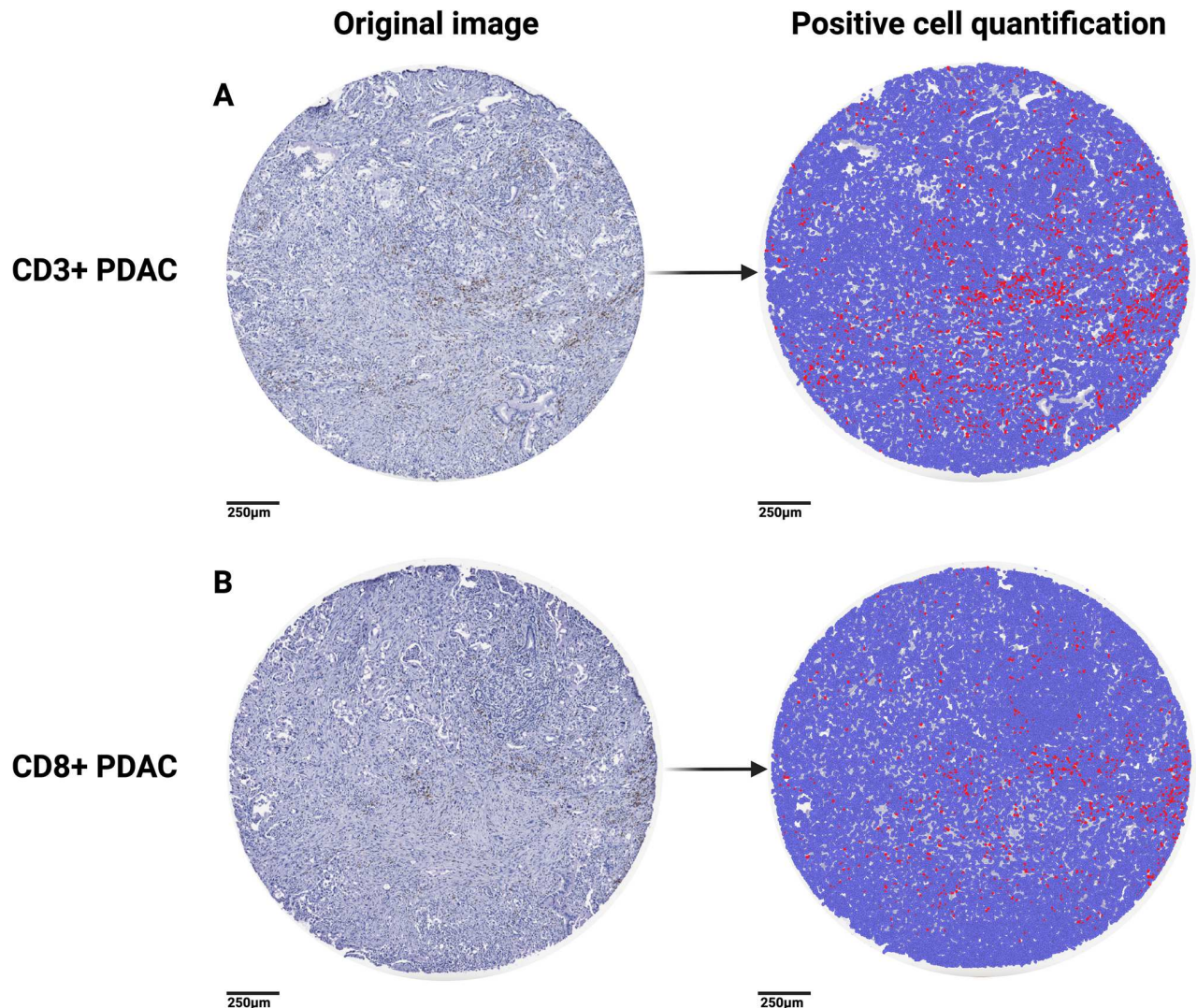
Statistical analysis

All statistical analyses were performed in the software GraphPad Prism 9.4.1. Shapiro-Wilk tests of the lymphocyte count and inflammatory protein levels in each tumor was used to assess normality and distribution. Due to non-normally distributed data observed in both lymphocyte cell counts and soluble protein analysis, non-parametric tests were used. Mann-Whitney U test was used to compare cell counts and infiltrating lymphocyte levels across tissues, and Spearman correlation was used to assess associations. Multivariate regression was used to assess relationships between clinicopathologic characteristics (i.e., CD3+% and age) in addition to spearman correlations. Kaplan-Meier method was employed to evaluate differences in overall survival. Spearman correlation analyses were performed between the percent of CD3 +/CD8+ cells and all 41 analytes in paired tumors or tissue. Data is presented as medians. A two-tailed P-value <0.05 is considered statistically significant.

Results

Quantitative analysis of intratumoral CD3+ and CD8+ lymphocytes in PDAC

The constructed TMA (prior to quality assurance) consisted of 59 treatment naïve pancreatic cancers and 37 non-PDAC controls. Clinicopathological characteristics are noted in Table 1. TMAs were immunohistochemically stained for CD3+ lymphocytes and CD8+ lymphocytes in duplicates. Our pathologist reviewed each TMA for quality assurance and semi-quantitatively graded the staining intensity in a blinded fashion. For quantitative assessment, cell counting was performed using the software package QuPath [8]. Following quality assurance, 56 PDAC tumors and 21 non-PDAC samples were analyzed in the CD3+ TMA, and 59 PDAC tumors and 24 non-PDAC samples were analyzed in the CD8+ TMA. The analyzable non-PDAC group included pancreatitis (n = 12), IPMN (n = 3), and other tissue (3 mucinous cystic neoplasm, 2 pancreatic neuroendocrine tumor, 1 pseudopapillary neoplasm) in the CD3 TMA. And the analyzable non-PDAC group for the CD8 TMA included pancreatitis (n = 13), IPMN (n = 4), and other (4 mucinous cystic neoplasm, 1 pancreatic neuroendocrine tumor, 1 squamoid cyst, and 1 pseudopapillary neoplasm).

PDAC displayed noteworthy heterogeneity in its CD3+ and CD8+ populations. Serial sections of tumor resulted in varying levels of CD3+ (Fig 1a) and CD8+ (Fig 1b) cells. To account for this, we created duplicate TMAs for each core, and, when possible, averaged the percent positive between the groups. We noted that the distribution of CD3+ and CD8+ lymphocytes in the PDAC tumors were distributed relatively evenly (not clustered). Non-PDAC pancreas maintained high cell density characteristic of normal pancreas, as opposed to the less dense, desmoplastic reactions that forms in tumors (Fig 2a and 2c). We observed significant increases in CD3+ and CD8+ populations (by percentages, and absolute values) in PDAC tumors compared to non-PDAC control tissues with the exception of PDAC vs. IPMN, however, this may

Original image

Positive cell quantification

A

CD3+ PDAC

250µm

250µm

B

CD8+ PDAC

250µm

250µm

Fig 1. Quantification of intratumoral CD3+ and CD8+ lymphocytes. Representative samples of immunohistochemical staining of tumor cores, slices originate from the same tumor: (A) CD3+ PDAC and subsequent quantification, and (B) CD8+ PDAC and subsequent quantification. Blue-colored cells represent cells labelled negative, red-colored cells represent cells considered positive.

https://doi.org/10.1371/journal.pone.0297325.g001

be due to limited sample size of the IPMN cohort (Fig 2b and 2d). As expected, Spearman r correlation of CD3+ and CD8+ revealed a significant correlation (Fig 2e). Analysis of covariates (CD3/CD8 infiltration, age, sex, histologic grade) in a multi-variable linear regression revealed no correlation, and poor model fit (S1 Table). This has also been shown in previous studies [16]. Spearman correlation of individual covariates (age, sex, histologic grade) also showed no correlation (S1 Table).

Semi-quantitative and quantitative assessments and overall survival

We then compared quantitative analysis to semi-quantitative pathological grading to observe patterns between systematic scoring and quantitative techniques. As above, the TMAs were subject to evaluation by an independent pathologist and graded according to standard pathology guidelines (score 0–3). Individual cores were assessed, and duplicate TMA cores were
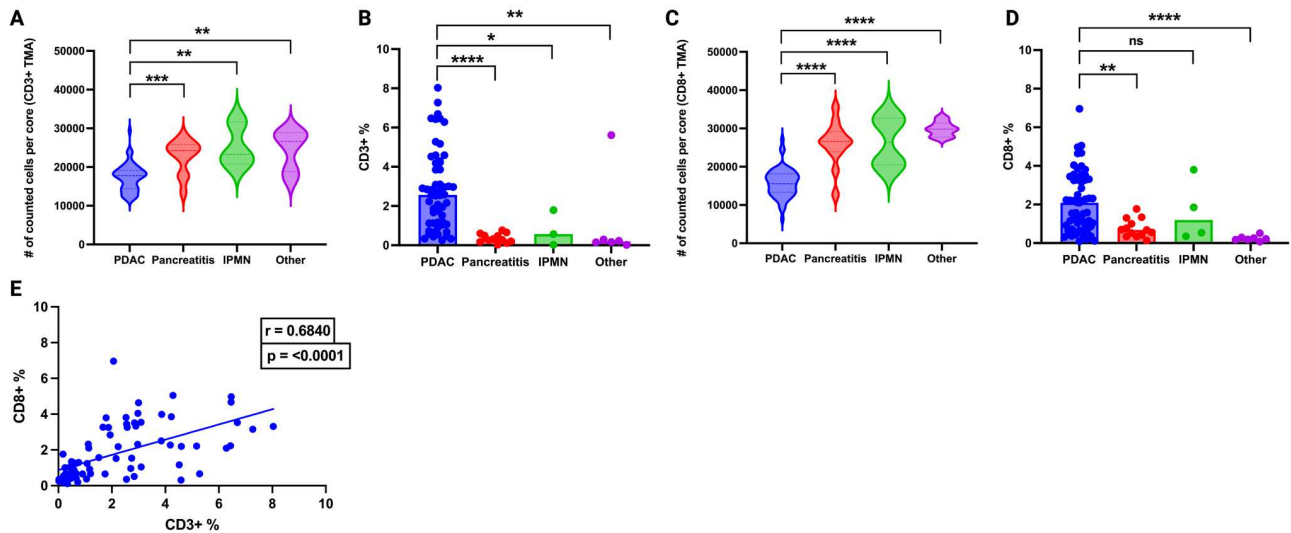
Fig 2. Assessment of intratumoral CD3+ and CD8+ lymphocyte populations. (A) Cell count of CD3+ TMA, PDAC (n = 56, median = 17785), Pancreatitis (n = 12, median = 24219), IPMN (n = 3, mean = 23315), Other (n = 6, mean = 26582), Mann Whitney U tests of PDAC vs Pancreatitis (p = 0.0003); PDAC vs IPMN (p = 0.0041); PDAC vs Other (p = 0.0031). (B) Prevalence of CD3+ lymphocytes in PDAC (n = 56, median = 2.565%), Pancreatitis (n = 12, median = 0.2950%), IPMN (n = 3, median = 0.5628%), Other (n = 6, median = 0.1919%). Mann-Whitney test of PDAC vs Pancreatitis (p = <0.0001), PDAC vs IPMN (p = 0.0434), PDAC vs other (p = 0.0031). (C) Cell count of CD8+ TMA, PDAC (n = 59, median = 15569), Pancreatitis (n = 13, median = 26580), IPMN (n = 4, median = 26355), Other (n = 7, median = 29877). (D) Prevalence of CD8+ lymphocytes in PDAC (n = 59, median = 2.090%), Pancreatitis (n = 13, median = 0.6800%), IPMN (n = 4, median = 1.195%), Other (n = 7, median = 0.2200%). Mann-Whitney test of PDAC vs Pancreatitis (p = 0.0018), PDAC vs IPMN (p = 0.5012), PDAC vs Other (p = <0.0001). (E) Correlation of CD3+ and CD8 + lymphocyte percentages of PDAC and non-PDAC in the TMAs, r = 0.684 and p = <0.0001.

https://doi.org/10.1371/journal.pone.0297325.g002

used individually (as opposed to averaged values) to appropriately, and directly, assess grading and quantification conversion. Fig 3A and 3C visually demonstrate the impact of conversion from integer semi-quantification to continuous variable data from the digital quantification. To assess the prognostic value of CD3+ and CD8+ infiltration and compare differences in grading and quantification, we performed Kaplan-Meier tests. We split the cohort at the median, thus CD3+ or CD8+ low tumors from the bottom 50th percentile for cell count versus CD3+ or CD8+ high tumors from the top 50th percentile group. Survival by quantitative grading was split into three groups, 0, 1, 2. No tumors were graded as 3. In our survival comparison, grades of 0 were compared with the tumors with "low" infiltration, and grades of 1 or 2 were compared with tumors with "high" infiltration.

We did not observe a significant difference in overall survival between CD3+ low and high groups through quantitative technique, with a median survival of 273 days in CD3+ low tumors, and 642.5 days in CD3+ high tumors (p = 0.2184). Pathological grading for CD3 + cores demonstrated a statistical significance between 0 and 1 grades. CD3+ cores graded 0 demonstrated a median survival of 252 days, CD3+ cores graded 1 had a median survival of 778 days (p = 0.0017) (Fig 3b). No statistically significant differences in survival were found in grading vs. quantitative technique, CD3 low vs. 0 (p = 0.1907), and CD3 high vs. 1 (p = 0.7003) No cores in the CD3+ group were graded 2.

We observed a significant difference between CD8+ low and CD8+ high tumors, with a median survival of 240 days, and 1059 days, respectively (p = 0.0003). CD8+ tumors with grades 0, 1, 2, also demonstrated statistically significance, with a median overall survival of 240 days, 642 days, and 951 days, respectively (p = 0.0156) (Fig 3d). Comparison of grading and quantitative technique found no significant differences between CD8+ low vs. 0 (p = 0.7982), CD8+ high vs. 1 (p = 0.6887), and CD8+ high vs 2 (p = 0.5882). Taken together, this data
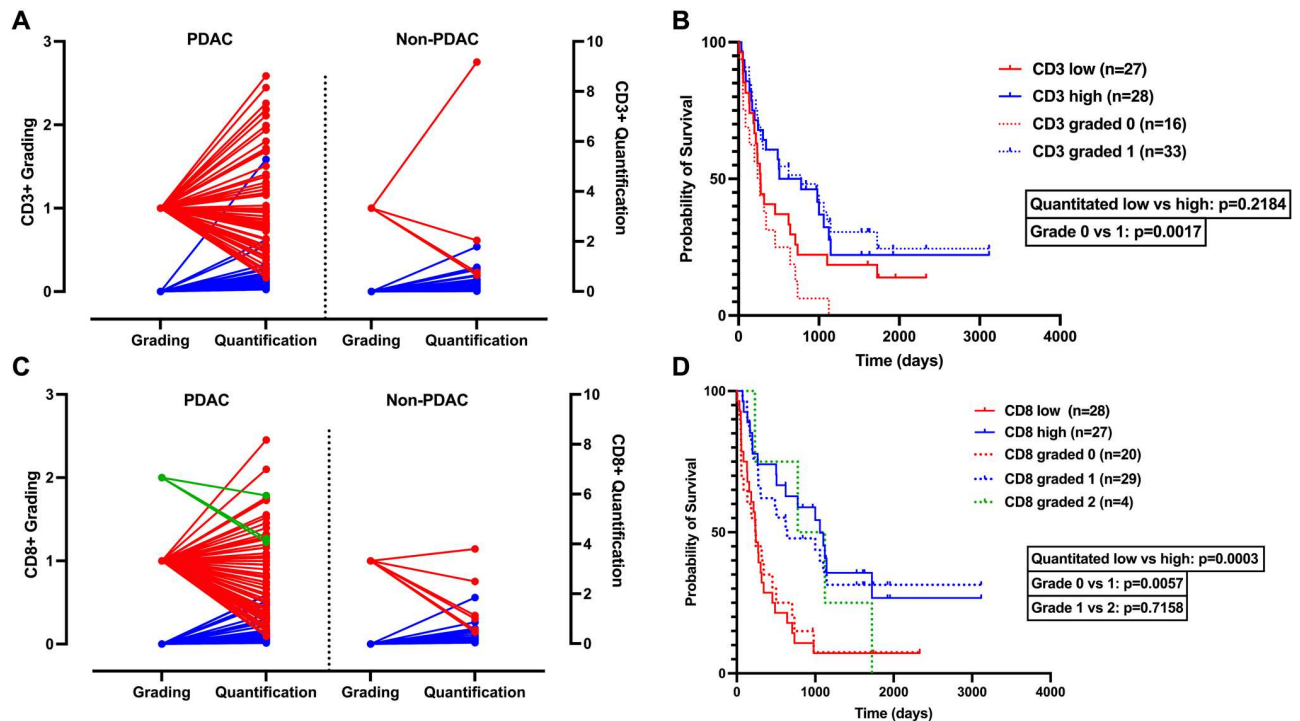
Fig 3. Comparison of semi-quantitative and quantitative assessments of CD3+ and CD8+ lymphocytes in association with overall survival. (A) Comparison of semiquantitative grading of cores with quantitative assessment for CD3+ staining (blue lines represent a grade of 0, red lines represent a grade of 1, green lines represent a grade of 2). In the CD3+ TMA, 99 individual cores in the PDAC group, and 36 cores in the non-PDAC group were graded and quantitated. (B) CD3+ overall survival comparison of quantitative methods vs grading method (CD3+ low = solid red, CD3+ high = solid blue, 0 = dashed red line, 1 = dashed blue line). CD3+ low tumors had a median survival of 273 days, and a median survival of 642.5 days in CD3+ high tumors (p = 0.2184). CD3+ cores graded 0 demonstrated a median survival of 252 days, CD3+ cores graded 1 had a median survival of 778 days (p = 0.0017). In comparing grading vs. quantitative technique, no statistically significant difference was found; CD3 low vs. 0 (p = 0.1907), and CD3 high vs. 1 (p = 0.7003). (C) Comparison of semi-quantitative grading of cores converted to quantitative assessment for CD8+ staining. In the CD8 + TMA, 90 individual cores and 37 non-PDAC cores were graded and quantitated. (D) CD8+ overall survival comparison of quantitative methods vs grading method. CD8+ low tumors had a median survival of 240 days, CD8+ high tumors had a median survival of 1059 days (p = 0.0003). CD8 + tumors with grade 0 vs 1 had a median survival of 240 days and 642 days (p = 0.0057), and grade 1 vs 2 had a median survival of 642 and 951 days (p = 0.7158). Grading vs. quantitative technique showed no significant differences, CD8+ low vs 0 (p = 0.7982), CD8+ high vs 1 (p = 0.6887), CD8 + high vs 2 (p = 0.5882).

shows how a quantitative approach may provide more precise, continuous data that does not necessarily result in superior prognostication in this relatively small sample set.

Identification of an inflammatory protein signature in PDAC with increased CD3+ and CD8+ infiltration

Inflammatory signaling mediates the activation and recruitment of cells to the tumor site [17,18]. We hypothesized that CD3+ high tumors and CD8+ high tumors had distinct tumor microenvironment inflammatory milieus. To test this, we performed a multiplex analysis of 41 inflammatory analytes with subsequent Spearman correlation analyses to find associations between these analytes and levels of CD3+ (Fig 4a) or CD8+ (Fig 5a) infiltration in PDAC. We performed a principal component analysis (PCA) of CD3+ PDAC, pancreatitis, IPMN and other miscellaneous tissue. Principal component analysis (PCA) used 31 analytes, as data from 10 analytes (G-CSF, IL-9, IL-1B, IL-2, IL-3, IL-4, IL-5, MIP-1A, RANTES, and TNFB) were non-informative (Figs 4d and 5c). PCA visually demonstrates the diversity of inflammatory signatures and notable heterogeneity in PDAC, with some PDAC showing overlap between
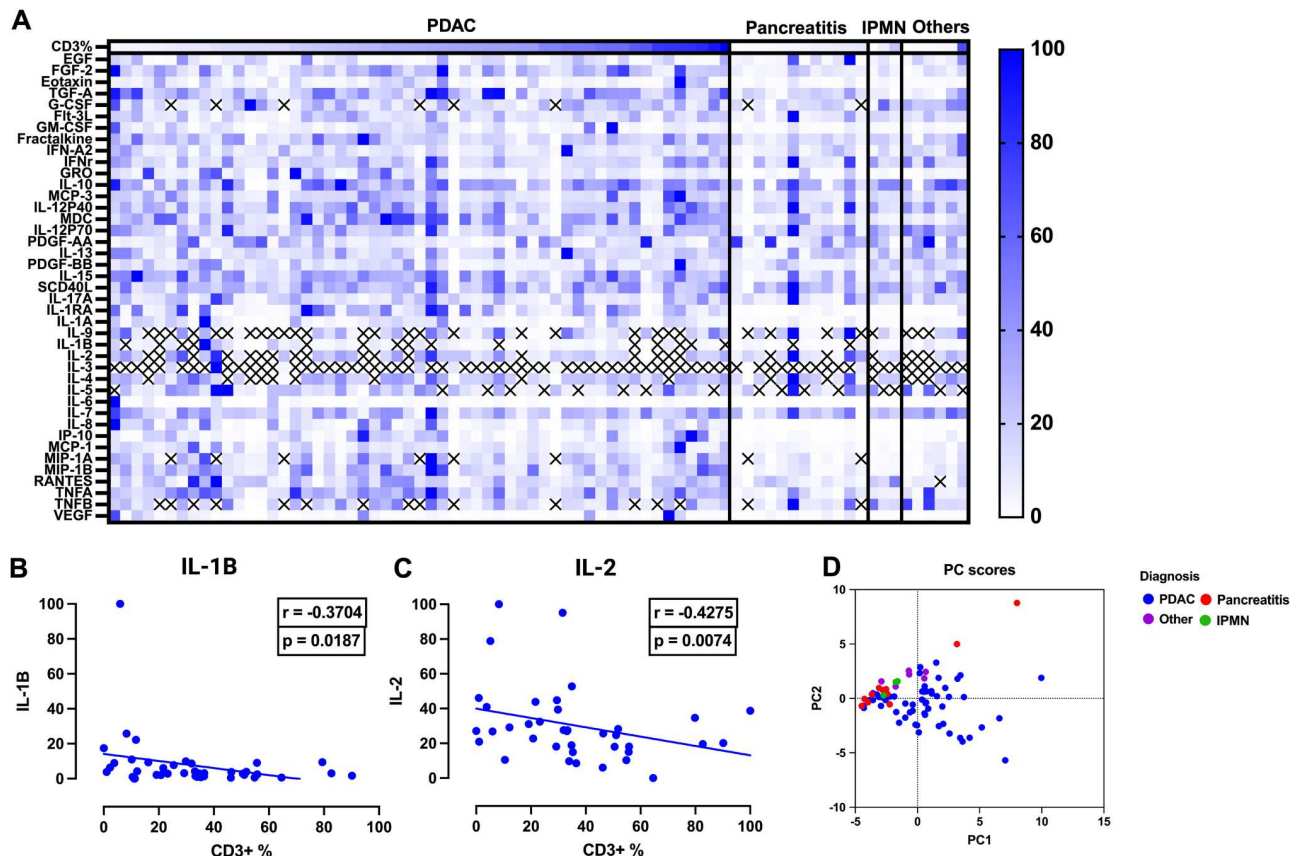
Fig 4. Expression of cytokines by CD3+ infiltration in PDAC. (A) Heatmap of 41 analytes in PDAC (n = 55) and non-PDAC tissue (Pancreatitis (n = 12), IPMN (n = 3), Other (n = 6)), expression levels were normalized to protein concentration (B, C): Spearman correlation analysis of IL-1B (r = -0.3704, p = 0.0187) and IL-2 (r = -0.4275, p = 0.0074) show decreased concentrations were significantly associated with increased CD3+ infiltration. (D) Principal component analysis plot of inflammatory signatures in different tissues, PCA was performed using 31 analytes, as 10 analytes (G-CSF, IL-9,IL-1B,IL-2,IL-3,IL-4,IL-5,MIP-1A,RANTES and TNFB) had limited detection across our patient cohort. PDAC (blue) is noted to be heterogenous in its inflammatory profile compared to non-PDAC tissue (Pancreatitis = red, Other = purple, IPMN = green).

https://doi.org/10.1371/journal.pone.0297325.g004

IPMN and non-PDAC signatures. Out of 41 inflammatory proteins analyzed (Table 2) We found higher levels of IL-1B and IL-2 to be significantly correlated with lower CD3+ infiltration, r = -0.3704, -0,4275, with p = 0.0187, 0.0074, respectively (Fig 4b and 4c).

We next aimed to identify inflammatory proteins associated with CD8+ infiltration. PCA was performed using 31 analytes as mentioned above. The PCA similarly shows high variability in the presence of inflammatory proteins in tumors, and some overlap between non-PDAC (Fig 5c). Of the 41 inflammatory proteins assessed (Table 3), only IL-1B demonstrated statistical significance and was associated with decreased CD8+ infiltration (r = -0.4299, p = 0.0045) (Fig 5b).

Discussion

In this work, we digitally measured intratumoral CD3+ and CD8+ lymphocytes and confirmed its effectiveness in the quantitative assessment of T-cell infiltration, which is predictive of overall survival in PDAC. PDAC demonstrated increased CD3+ and CD8+ infiltration compared to non-PDAC controls, and substantial heterogeneity. We found a significant increase in overall survival with high levels of CD8+ infiltration, but not CD3+ infiltration. We
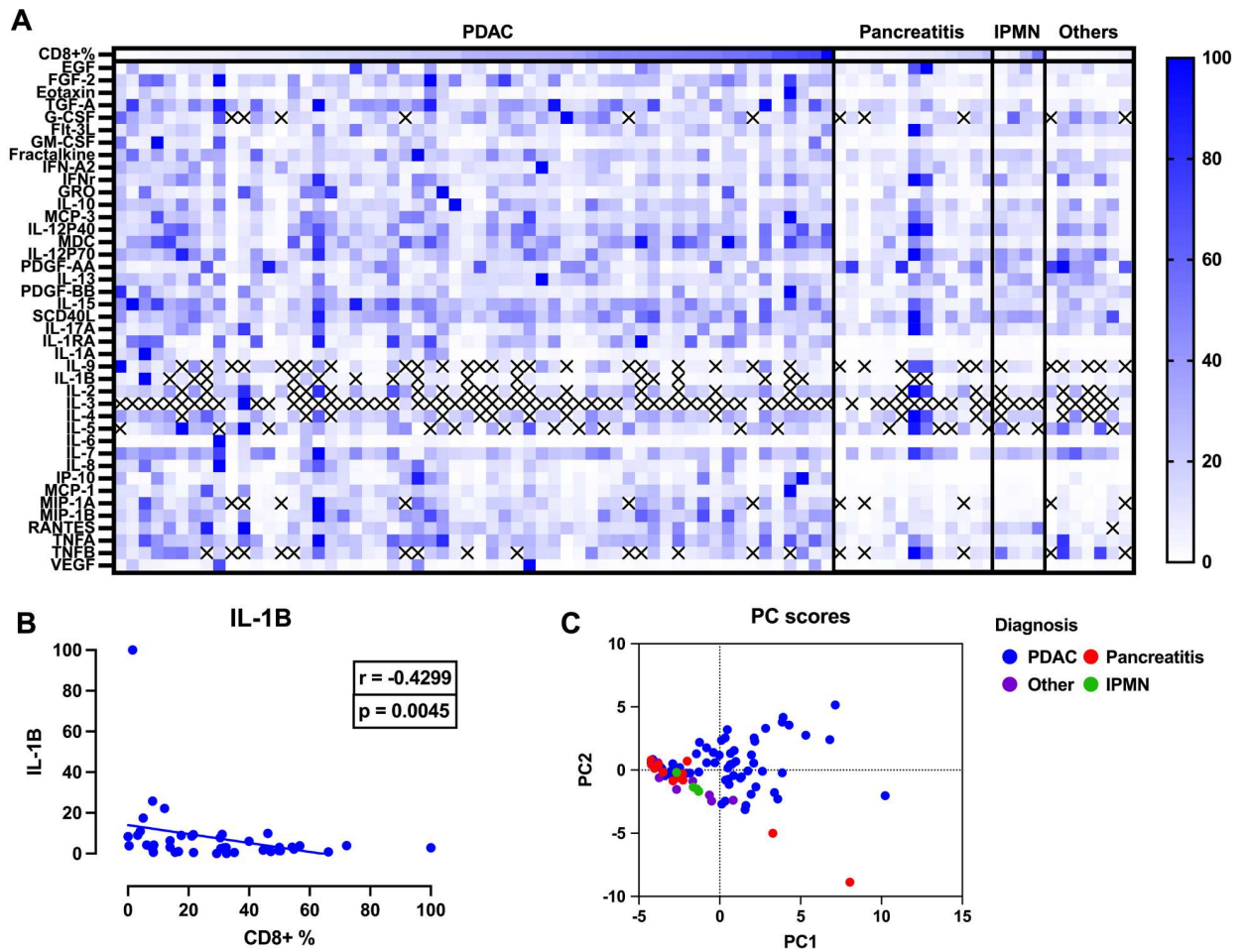
Fig 5. Expression of cytokines by CD8+ infiltration in PDAC. (A) Expression of 41 analytes in PDAC (n = 58) and non-PDAC (Pancreatitis (n = 13), IPMN (n = 4), Other (n = 7)) expression is normalized to protein concentration (B) Spearman correlation analyses showing increased expression of IL-1B significantly associated with decreased CD8+ infiltration (r = -0.4299, p = 0.0045). (C) Principal component analysis plot of inflammatory signatures in different tissues, PCA was performed using 31 analytes, as 10 analytes (G-CSF, IL-9,IL-1B,IL-2,IL-3,IL-4,IL-5,MIP-1A, RANTES and TNFB) had limited detection across our patient cohort. PDAC (blue) is noted to be heterogenous in its inflammatory profile compared to non-PDAC tissue (Pancreatitis = red, Other = purple, IPMN = green).

https://doi.org/10.1371/journal.pone.0297325.g005

further demonstrated correlations between inflammatory protein signatures and levels of CD3 + and CD8+ infiltration.

Previous studies have used a range of approaches to evaluate the presence of CD3+ and CD8 + lymphocytes in tumors, including both quantitative and semiquantitative methods [19]. In this study, we contributed a standardized and reproducible method for quantifying CD3+ and CD8+ T-cells within a treatment-naïve patient cohort with PDAC. Semi-quantitative grading and quantitative approach through QuPath demonstrated similar outcomes in both prevalence of lymphocyte infiltration, and prognosis. The limited sample size in tumor or tissue graded 2 or 3 may limit the generalizability of these findings, and this analysis should be reproduced in tumors with expectantly higher lymphocyte infiltration, such as melanoma or microsatellite instable solid tumors. Through the identification of patients with objectively higher levels of CD8+ infiltration, we may be able to more effectively select patients who are most likely to benefit from immune-based therapies, such as checkpoint inhibitors or adoptive cell transfer.

Table 2. Correlation of CD3+ infiltration and chemokines/cytokines.

Immune cell type	Cytokine/chemokine	# of XY pairs	Spearman r	95% confidence	p-value
CD3	EGF	55	-0.0008658	-0.2736 to 0.2719	0.995
CD3	FGF-2	55	0.08615	-0.1911 to 0.3507	0.5317
CD3	Eotaxin (CCL11)	55	-0.1139	-0.3750 to 0.1640	0.4079
CD3	TGF-A	55	-0.01465	-0.2863 to 0.2591	0.9155
CD3	G-CSF	49	0.04684	-0.2455 to 0.3314	0.7493
CD3	Flt-3L	55	0.1027	-0.1750 to 0.3652	0.4557
CD3	GM-CSF	55	-0.1841	-0.4350 to 0.09331	0.1784
CD3	Fractalkine (CX3CL1)	55	-0.04192	-0.3111 to 0.2335	0.7612
CD3	IFN-A2	55	0.01053	-0.2630 to 0.2825	0.9392
CD3	IFNr	55	0.08268	-0.1945 to 0.3476	0.5484
CD3	GRO (CXCL1)	55	-0.1622	-0.4165 to 0.1157	0.2368
CD3	IL-10	55	0.1274	-0.1506 to 0.3867	0.3539
CD3	MCP-3 (CCL7)	55	-0.07446	-0.3403 to 0.2024	0.589
CD3	IL-12P40	55	0.06674	-0.2098 to 0.3334	0.6283
CD3	MDC (CCL22)	55	0.08312	-0.1940 to 0.3480	0.5463
CD3	IL-12P70	55	-0.05887	-0.3264 to 0.2174	0.6694
CD3	PDGF-AA	55	-0.01847	-0.2898 to 0.2556	0.8935
CD3	IL-13	55	0.07727	-0.1997 to 0.3428	0.575
CD3	PDGF-BB	55	-0.1454	-0.4022 to 0.1326	0.2896
CD3	IL-15	55	-0.1506	-0.4067 to 0.1273	0.2723
CD3	SCD40L	55	0.1591	-0.1188 to 0.4139	0.246
CD3	IL-17A	55	-0.02734	-0.2979 to 0.2472	0.8429
CD3	IL-1RA	55	0.01053	-0.2630 to 0.2825	0.9392
CD3	IL-1A	55	-0.1569	-0.4120 to 0.1210	0.2526
CD3	IL-9	32	-0.1276	-0.4645 to 0.2416	0.4866
CD3	IL-1B	40	-0.3704	-0.6173 to -0.05703	0.0187*
CD3	IL-2	38	-0.4275	-0.6629 to -0.1152	0.0074*
CD3	IL-3	6	-0.6	NA	0.2417
CD3	IL-4	46	-0.09504	-0.3826 to 0.2093	0.5298
CD3	IL-5	46	-0.1023	-0.3888 to 0.2022	0.4987
CD3	IL-6	55	-0.2247	-0.4688 to 0.05114	0.099
CD3	IL-7	55	0.02027	-0.2539 to 0.2914	0.8832
CD3	IL-8 (CXCL8)	55	-0.1544	-0.4099 to 0.1236	0.2604
CD3	IP-10 (CXCL10)	55	0.08947	-0.1879 to 0.3536	0.516
CD3	MCP-1 (CCL2)	55	-0.1016	-0.3642 to 0.1760	0.4605
CD3	MIP-1A (CCL3)	49	-0.02959	-0.3159 to 0.2617	0.84
CD3	MIP-1B (CCL4)	55	0.009596	-0.2638 to 0.2816	0.9446
CD3	RANTES (CCL5)	55	-0.03896	-0.3084 to 0.2363	0.7776
CD3	TNFA	55	-0.0386	-0.3081 to 0.2366	0.7796
CD3	TNFB	41	-0.0899	-0.3948 to 0.2329	0.5762
CD3	VEGF	55	-0.1509	-0.4069 to 0.1270	0.2713

While PDAC has been shown to be resistant to current immunotherapeutics, recruitment and activation of T-cells into the tumor site may still be a viable approach [20,21]. Individual inflammatory molecules have been leveraged to guide immune cells into the tumor-microenvironment [22,23], however, a multifaceted approach to modifying inflammation, involving multiple inflammatory molecules, may result in improved immunogenicity in pancreatic

Table 3. Correlation of CD8+ infiltration and chemokines/cytokines.

Immune cell type	Cytokine/chemokine	# of XY pairs	Spearman r	95% confidence	p-value
CD8	EGF	58	0.1222	-0.1482 to 0.3755	0.361
CD8	FGF-2	58	0.1275	-0.1429 to 0.3802	0.3403
CD8	Eotaxin (CCL11)	58	-0.03522	-0.2980 to 0.2325	0.793
CD8	TGF-A	58	-0.08884	-0.3462 to 0.1810	0.5072
CD8	G-CSF	52	-0.001964	-0.2824 to 0.2787	0.989
CD8	Flt-3L	58	0.1486	-0.1218 to 0.3984	0.2657
CD8	GM-CSF	58	-0.1146	-0.3690 to 0.1557	0.3915
CD8	Fractalkine (CX3CL1)	58	-0.08213	-0.3403 to 0.1875	0.5399
CD8	IFN-A2	58	-0.1331	-0.3851 to 0.1373	0.3191
CD8	IFNr	58	0.03857	-0.2293 to 0.3011	0.7737
CD8	GRO (CXCL1)	58	-0.1366	-0.3881 to 0.1338	0.3065
CD8	IL-10	58	0.01781	-0.2489 to 0.2820	0.8944
CD8	MCP-3 (CCL7)	58	-0.02572	-0.2893 to 0.2415	0.848
CD8	IL-12P40	58	0.182	-0.08777 to 0.4270	0.1714
CD8	MDC (CCL22)	58	0.2436	-0.02346 to 0.4783	0.0653
CD8	IL-12P70	58	-0.1283	-0.3809 to 0.1421	0.337
CD8	PDGF-AA	58	-0.1466	-0.3967 to 0.1238	0.2722
CD8	IL-13	58	0.04411	-0.2241 to 0.3061	0.7423
CD8	PDGF-BB	58	-0.199	-0.4413 to 0.07026	0.1342
CD8	IL-15	58	-0.1433	-0.3939 to 0.1271	0.2832
CD8	SCD40L	58	0.1694	-0.1007 to 0.4162	0.2036
CD8	IL-17A	58	-0.0474	-0.3091 to 0.2210	0.7238
CD8	IL-1RA	58	0.1378	-0.1326 to 0.3891	0.3023
CD8	IL-1A	58	-0.1898	-0.4335 to 0.07977	0.1535
CD8	IL-9	35	-0.244	-0.5411 to 0.1073	0.1578
CD8	IL-1B	42	-0.4299	-0.6544 to -0.1358	0.0045*
CD8	IL-2	41	-0.007753	-0.3231 to 0.3091	0.9616
CD8	IL-3	6	-0.3143	NA	0.5639
CD8	IL-4	49	-0.08429	-0.3645 to 0.2099	0.5647
CD8	IL-5	47	-0.2104	-0.4760 to 0.09037	0.1557
CD8	IL-6	58	-0.1514	-0.4008 to 0.1190	0.2567
CD8	IL-7	58	-0.1971	-0.4396 to 0.07227	0.1381
CD8	IL-8 (CXCL8)	58	-0.1671	-0.4143 to 0.1030	0.2099
CD8	IP-10 (CXCL10)	58	0.04427	-0.2239 to 0.3062	0.7414
CD8	MCP-1 (CCL2)	58	-0.1098	-0.3648 to 0.1604	0.4117
CD8	MIP-1A (CCL3)	52	0.05182	-0.2321 to 0.3276	0.7152
CD8	MIP-1B (CCL4)	58	0.03916	-0.2288 to 0.3016	0.7704
CD8	RANTES (CCL5)	58	0.08416	-0.1856 to 0.3421	0.5299
CD8	TNFA	58	0.003045	-0.2627 to 0.2684	0.9819
CD8	TNFB	44	-0.2149	-0.4880 to 0.09650	0.1612
CD8	VEGF	58	-0.2038	-0.4453 to 0.06531	0.1249

cancer [24]. In this study, we established connections between T-cells, effector T-cells and inflammatory molecules in order to identify potential candidates that could aid in the immune recognition of PDAC.

The recruitment and activation of immune cells into the tumor microenvironment is fundamental to the success of immunotherapy. Our findings, as well as others, illustrated the

importance of tumor-derived cytokines in lymphocyte recruitment [25–28]. Factors secreted by cancer cells, such as GM-CSF and G-CSF have been reported to be associated with the recruitment of leukocytes into the TME [26,29]. Additionally, cytokines have been identified as mediators of therapeutic resistance in PDAC [30]. These cytokines remodel ambient cell populations to create a tumor permissive environment. Infiltration of T-cells in solid tumors have been associated with superior survival, however, in PDAC, populations of intratumor T-cells are scarce and are often unable to mount an effective anti-tumor immune response [31]. IL-1B has been shown to promote tumor survival, proliferation, and metastatic potential [32]. IL-1B also influences the tumor microenvironment by enhancing desmoplasia and immune suppression in pancreas and breast cancer [32–34]. IL-2 is a cytokine responsible for the growth, proliferation, and survival of T-cells. IL-2 has been shown to play a vital role in the regulation of CD8+ T-cells to maintain their reactivity against tumor cells [35,36]. Our data suggests that IL-1B may play a more dominant role in regulating T-cell recruitment into the tumor microenvironment. We posit that IL-2's role is more nuanced, potentially contributing to the activation and exhaustion of T-cells or effecting other T-cell subtypes and immune cells [37]. A more precise method for remodeling the tumor microenvironment may be achievable though spatial analysis of the microenvironment with respect to the secretion of inflammatory proteins and lymphocyte involvement. We previously reported differences in the transcriptome of cancer-associated fibroblasts based on proximity to tumor [38], these changes may be mediated by surrounding inflammatory molecules. In immune-hot solid tumors that respond well to immune checkpoint inhibitors, such as melanoma, T-cell and other immune cells that are recruited into the tumor-microenvironment are essential to mounting an effective immune response [39]. We speculate that there are inflammatory characteristics of CD3+ or CD8 + abundant tumors that can be exploited with tumors with less immunogenicity.

The heterogeneity of the pancreatic tumor microenvironment has posed challenges for both treatment and study [40–42]. In our study, we aimed to minimize variability by only including treatment naïve PDAC patients. Yet, we still observed significant heterogeneity in both the CD3+ and CD8+ populations and in the levels of inflammatory molecules across samples. We reported limited detection of certain cytokines (G-CSF, IL-9, IL-1B, IL-2, IL-3, IL-4, IL-5, MIP-1A, RANTES, and TNFB), though these cytokines may still be useful for further investigation. While our exploratory analysis found significant associations between IL-1B and IL-2 and lymphocyte infiltration, there is a need for additional mechanistic study to exploit the inflammatory axis to induce immune response to tumor. Future studies with larger validation cohorts that are more representative of the patient population could greatly improve our understanding of inflammation in PDAC and other solid tumor malignancies. Assessing the location of lymphocytes and inflammatory proteins (i.e., central tumor or tumor margin) may also prove useful to increase infiltration and penetration of lymphocytes in solid tumors. The relatively small sample size, and the fact that the patient cohort used in our analysis consisted largely of T-stage III tumors, may limit generalizability of our findings. A larger sample size, from various stages of tumor progression that assess whole tumor may provide greater statistical power, reduce the risk of type II errors, and allow for additional subgroup analyses.

Cancer cells employ pro/anti-inflammatory cytokines and chemokines to suppress or promote an immune-rich microenvironment [43–45]. The presence or absence of these cytokines can dictate local cell populations and ultimately the host's response to malignancy. Here, we found that increased levels of IL-1B and IL-2 were associated with lowered CD3+ T-cell infiltration, and increased IL-1B was associated with decreased CD8+ T-cell populations. Solid-tumor malignancies, such as PDAC, have a particularly inflexible scaffolding in the form of stroma that add an additional physical barrier to limit immune-cell involvement and sensitivity to traditional therapeutics [46,47]. Ongoing clinical trials are utilizing cytokines as vehicles

to increase tumor immunogenicity and remodeling the tumor microenvironment [48]. Our study combines advances in intratumoral immune cell quantification and characterization of inflammatory components to advance our understandings of the PDAC tumor microenvironment.

Supporting information

S1 Table. Comparisons of infiltrating CD3+ and CD8+ lymphocytes and covariate analysis.
(XLSX)

S2 Table. Dataset of patient cohort, CD3+ and CD8+ lymphocyte quantification, and inflammatory assay.
(XLSX)

Acknowledgments

We would like to thank Dr. Dongtao Ann Fu, Cathy Yuping Sun, and the University of Florida Molecular Pathology Core (RRID:SCR_016601) for assistance with TMA assembly, staining, and scanning. We would also like to acknowledge the contributions of our patients and their families for enabling us to advance our understanding of pancreatic cancer.

Author Contributions

Conceptualization: Gerik W. Tushoski-Alemán.

Data curation: Gerik W. Tushoski-Alemán, Kelly M. Herremans, Patrick W. Underwood, Ashwin Akki.

Formal analysis: Gerik W. Tushoski-Alemán, Ashwin Akki.

Funding acquisition: Jose G. Trevino, Steven J. Hughes.

Investigation: Gerik W. Tushoski-Alemán, Ashwin Akki, Song Han.

Methodology: Gerik W. Tushoski-Alemán, Ashwin Akki, Song Han, Steven J. Hughes.

Project administration: Jose G. Trevino, Song Han, Steven J. Hughes.

Resources: Kelly M. Herremans, Patrick W. Underwood, Jose G. Trevino, Steven J. Hughes.

Supervision: Song Han, Steven J. Hughes.

Validation: Gerik W. Tushoski-Alemán, Kelly M. Herremans, Song Han, Steven J. Hughes.

Visualization: Gerik W. Tushoski-Alemán, Kelly M. Herremans, Andrea N. Riner, Song Han, Steven J. Hughes.

Writing – original draft: Gerik W. Tushoski-Alemán, Kelly M. Herremans, Patrick W. Underwood, Ashwin Akki, Andrea N. Riner, Song Han, Steven J. Hughes.

Writing – review & editing: Gerik W. Tushoski-Alemán, Kelly M. Herremans, Patrick W. Underwood, Ashwin Akki, Andrea N. Riner, Song Han, Steven J. Hughes.

References

1. Siegel RL, Miller KD, Fuchs HE, Jemal A. Cancer statistics, 2022. CA Cancer J Clin. 2022; 72: 7–33. https://doi.org/10.3322/caac.21708 PMID: 35020204

2. Delitto D, Wallet SM, Hughes SJ. Targeting tumor tolerance: A new hope for pancreatic cancer therapy? Pharmacol Ther. 2016; 166: 9–29. https://doi.org/10.1016/j.pharmthera.2016.06.008 PMID: 27343757

3. Somani VK, Zhang D, Dodhiawala PB, Lander VE, Liu X, Kang L-I, et al. IRAK4 Signaling Drives Resistance to Checkpoint Immunotherapy in Pancreatic Ductal Adenocarcinoma. Gastroenterology. 2022; 162: 2047–2062. https://doi.org/10.1053/j.gastro.2022.02.035 PMID: 35271824

4. Purohit A, Saxena S, Varney M, Prajapati DR, Kozel JA, Lazenby A, et al. Host Cxcr2-Dependent Regulation of Pancreatic Cancer Growth, Angiogenesis, and Metastasis. Am J Pathol. 2021; 191: 759–771. https://doi.org/10.1016/j.ajpath.2021.01.002 PMID: 33453178

5. Lafaro KJ, Melstrom LG. The Paradoxical Web of Pancreatic Cancer Tumor Microenvironment. Am J Pathol. 2019; 189: 44–57. https://doi.org/10.1016/j.ajpath.2018.09.009 PMID: 30558722

6. Erez N, Truitt M, Olson P, Hanahan D. Cancer-Associated Fibroblasts Are Activated in Incipient Neoplasia to Orchestrate Tumor-Promoting Inflammation in an NF-κB-Dependent Manner. Cancer Cell. 2010; 17: 135–147. https://doi.org/10.1016/j.ccr.2009.12.041 PMID: 20138012

7. Delitto D, Delitto AE, DiVita BB, Pham K, Han S, Hartlage ER, et al. Human Pancreatic Cancer Cells Induce a MyD88-Dependent Stromal Response to Promote a Tumor-Tolerant Immune Microenvironment. Cancer Res. 2017; 77: 672–683. https://doi.org/10.1158/0008-5472.CAN-16-1765 PMID: 27864347

8. Bankhead P, Loughrey MB, Fernández JA, Dombrowski Y, McArt DG, Dunne PD, et al. QuPath: Open source software for digital pathology image analysis. Sci Rep. 2017; 7: 16878. https://doi.org/10.1038/s41598-017-17204-5 PMID: 29203879

9. Duan K, Jang G-H, Grant RC, Wilson JM, Notta F, O'Kane GM, et al. The value of GATA6 immunohistochemistry and computer-assisted diagnosis to predict clinical outcome in advanced pancreatic cancer. Sci Rep. 2021; 11: 14951. https://doi.org/10.1038/s41598-021-94544-3 PMID: 34294813

10. Miles GJ, Powley I, Mohammed S, Howells L, Pringle Jhoward, Hammonds T, et al. Evaluating and comparing immunostaining and computational methods for spatial profiling of drug response in patient-derived explants. Laboratory Investigation. 2021; 101: 396–407. https://doi.org/10.1038/s41374-020-00511-3 PMID: 33318618

11. Dias Costa A, Väyrynen SA, Chawla A, Zhang J, Väyrynen JP, Lau MC, et al. Neoadjuvant Chemotherapy Is Associated with Altered Immune Cell Infiltration and an Anti-Tumorigenic Microenvironment in Resected Pancreatic Cancer. Clinical Cancer Research. 2022; 28: 5167–5179. https://doi.org/10.1158/1078-0432.CCR-22-1125 PMID: 36129461

12. Li K, Tandurella JA, Gai J, Zhu Q, Lim SJ, Thomas DL, et al. Multi-omic analyses of changes in the tumor microenvironment of pancreatic adenocarcinoma following neoadjuvant treatment with anti-PD-1 therapy. Cancer Cell. 2022; 40: 1374–1391.e7. https://doi.org/10.1016/j.ccell.2022.10.001 PMID: 36306792

13. Golesworthy B, Wang Y, Tanti A, Pacis A, Romero JM, Cuggia A, et al. Intra-Tumoral CD8+ T-Cell Infiltration and PD-L1 Positivity in Homologous Recombination Deficient Pancreatic Ductal Adenocarcinoma. Front Oncol. 2022; 12. https://doi.org/10.3389/fonc.2022.860767 PMID: 35547873

14. Loughrey MB, Bankhead P, Coleman HG, Hagan RS, Craig S, McCorry AMB, et al. Validation of the systematic scoring of immunohistochemically stained tumour tissue microarrays using QuPath digital image analysis. Histopathology. 2018; 73: 327–338. https://doi.org/10.1111/his.13516 PMID: 29575153

15. Underwood PW, Gerber MH, Nguyen K, Delitto D, Han S, Thomas RM, et al. Protein Signatures and Tissue Diagnosis of Pancreatic Cancer. J Am Coll Surg. 2020; 230: 26–36e1. https://doi.org/10.1016/j.jamcollsurg.2019.10.002 PMID: 31672677

16. Kiryu S, Ito Z, Suka M, Bito T, Kan S, Uchiyama K, et al. Prognostic value of immune factors in the tumor microenvironment of patients with pancreatic ductal adenocarcinoma. BMC Cancer. 2021; 21: 1197. https://doi.org/10.1186/s12885-021-08911-4 PMID: 34758773

17. Saxena S, Singh RK. Chemokines orchestrate tumor cells and the microenvironment to achieve metastatic heterogeneity. Cancer and Metastasis Reviews. 2021; 40: 447–476. https://doi.org/10.1007/s10555-021-09970-6 PMID: 33959849

18. Foeng J, Comerford I, McColl SR. Harnessing the chemokine system to home CAR-T cells into solid tumors. Cell Rep Med. 2022; 3: 100543. https://doi.org/10.1016/j.xcrm.2022.100543 PMID: 35492880

19. Moratin J, Mock A, Obradovic S, Metzger K, Flechtenmacher C, Zaoui K, et al. Digital Pathology Scoring of Immunohistochemical Staining Reliably Identifies Prognostic Markers and Anatomical Associations in a Large Cohort of Oral Cancers. Front Oncol. 2021; 11. https://doi.org/10.3389/fonc.2021.712944 PMID: 34395287

20. Raj D, Yang M-H, Rodgers D, Hampton EN, Begum J, Mustafa A, et al. Switchable CAR-T cells mediate remission in metastatic pancreatic ductal adenocarcinoma. Gut. 2019; 68: 1052–1064. https://doi.org/10.1136/gutjnl-2018-316595 PMID: 30121627

21. Bruchard M, Geindreau M, Perrichet A, Truntzer C, Ballot E, Boidot R, et al. Recruitment and activation of type 3 innate lymphoid cells promote antitumor immune responses. Nat Immunol. 2022; 23: 262–274. https://doi.org/10.1038/s41590-021-01120-y PMID: 35102345

22. Bellone G, Turletti A, Artusio E, Mareschi K, Carbone A, Tibaudi D, et al. Tumor-Associated Transforming Growth Factor-β and Interleukin-10 Contribute to a Systemic Th2 Immune Phenotype in Pancreatic Carcinoma Patients. Am J Pathol. 1999; 155: 537–547. https://doi.org/10.1016/S0002-9440(10)65149-8 PMID: 10433946

23. Lutz V, Hellmund VM, Picard FSR, Raifer H, Ruckenbrod T, Klein M, et al. IL18 Receptor Signaling Regulates Tumor-Reactive CD8+ T-cell Exhaustion via Activation of the IL2/STAT5/mTOR Pathway in a Pancreatic Cancer Model. Cancer Immunol Res. 2023; 11: 421–434. https://doi.org/10.1158/2326-6066.CIR-22-0398 PMID: 36758176

24. Tähtinen S, Kaikkonen S, Merisalo-Soikkeli M, Grönberg-Vähä-Koskela S, Kanerva A, Parviainen S, et al. Favorable Alteration of Tumor Microenvironment by Immunomodulatory Cytokines for Efficient T-Cell Therapy in Solid Tumors. PLoS One. 2015; 10: e0131242. https://doi.org/10.1371/journal.pone.0131242 PMID: 26107883

25. Marigo I, Bosio E, Solito S, Mesa C, Fernandez A, Dolcetti L, et al. Tumor-Induced Tolerance and Immune Suppression Depend on the C/EBPβ Transcription Factor. Immunity. 2010; 32: 790–802. https://doi.org/10.1016/j.immuni.2010.05.010 PMID: 20605485

26. Bayne LJ, Beatty GL, Jhala N, Clark CE, Rhim AD, Stanger BZ, et al. Tumor-Derived Granulocyte-Macrophage Colony-Stimulating Factor Regulates Myeloid Inflammation and T Cell Immunity in Pancreatic Cancer. Cancer Cell. 2012; 21: 822–835. https://doi.org/10.1016/j.ccr.2012.04.025 PMID: 22698406

27. Khajah M, Millen B, Cara DC, Waterhouse C, McCafferty D-M. Granulocyte-macrophage colony-stimulating factor (GM-CSF): a chemoattractive agent for murine leukocytes in vivo. J Leukoc Biol. 2011; 89: 945–953. https://doi.org/10.1189/jlb.0809546 PMID: 21393420

28. Herremans KM, Szymkiewicz DD, Riner AN, Bohan RP, Tushoski GW, Davidson AM, et al. The interleukin-1 axis and the tumor immune microenvironment in pancreatic ductal adenocarcinoma. Neoplasia. 2022; 28: 100789. https://doi.org/10.1016/j.neo.2022.100789 PMID: 35395492

29. Pylayeva-Gupta Y, Lee KE, Hajdu CH, Miller G, Bar-Sagi D. Oncogenic Kras-Induced GM-CSF Production Promotes the Development of Pancreatic Neoplasia. Cancer Cell. 2012; 21: 836–847. https://doi.org/10.1016/j.ccr.2012.04.024 PMID: 22698407

30. McAndrews KM, Chen Y, Darpolor JK, Zheng X, Yang S, Carstens JL, et al. Identification of Functional Heterogeneity of Carcinoma-Associated Fibroblasts with Distinct IL6-Mediated Therapy Resistance in Pancreatic Cancer. Cancer Discov. 2022; 12: 1580–1597. https://doi.org/10.1158/2159-8290.CD-20-1484 PMID: 35348629

31. Clark CE, Hingorani SR, Mick R, Combs C, Tuveson DA, Vonderheide RH. Dynamics of the Immune Reaction to Pancreatic Cancer from Inception to Invasion. Cancer Res. 2007; 67: 9518–9527. https://doi.org/10.1158/0008-5472.CAN-07-0175 PMID: 17909062

32. Das S, Shapiro B, Vucic EA, Vogt S, Bar-Sagi D. Tumor Cell–Derived IL1β Promotes Desmoplasia and Immune Suppression in Pancreatic Cancer. Cancer Res. 2020; 80: 1088–1101. https://doi.org/10.1158/0008-5472.CAN-19-2080 PMID: 31915130

33. Eyre R, Alférez DG, Santiago-Gómez A, Spence K, McConnell JC, Hart C, et al. Microenvironmental IL1β promotes breast cancer metastatic colonization in the bone via activation of Wnt signalling. Nat Commun. 2019; 10. https://doi.org/10.1038/s41467-019-12807-0 PMID: 31676788

34. Caronni N, La Terza F, Vittoria FM, Barbiera G, Mezzanzanica L, Cuzzola V, et al. IL-1β+ macrophages fuel pathogenic inflammation in pancreatic cancer. Nature. 2023; 623: 415–422. https://doi.org/10.1038/s41586-023-06685-2 PMID: 37914939

35. Shah P, Forget MA, Frank ML, Jiang P, Sakellariou-Thompson D, Federico L, et al. Combined IL-2, agonistic CD3 and 4-1BB stimulation preserve clonotype hierarchy in propagated non-small cell lung cancer tumor-infiltrating lymphocytes. J Immunother Cancer. 2022; 10. https://doi.org/10.1136/jitc-2021-003082 PMID: 35110355

36. Laporte KM, Hernandez R, Santos Savio A, Malek TR. Robust IL-2-dependent antitumor immunotherapy requires targeting the high-affinity IL-2R on tumor-specific CD8 + T cells. J Immunother Cancer. 2023; 11. https://doi.org/10.1136/jitc-2022-006611 PMID: 37270181

37. Liu Y, Zhou N, Zhou L, Wang J, Zhou Y, Zhang T, et al. IL-2 regulates tumor-reactive CD8+ T cell exhaustion by activating the aryl hydrocarbon receptor. Nat Immunol. 2021; 22: 358–369. https://doi.org/10.1038/s41590-020-00850-9 PMID: 33432230

38. Han S, Fu D, Tushoski GW, Meng L, Herremans KM, Riner AN, et al. Single-cell profiling of microenvironment components by spatial localization in pancreatic ductal adenocarcinoma. Theranostics. 2022; 12: 4980–4992. https://doi.org/10.7150/thno.73222 PMID: 35836806

39. Blando J, Sharma A, Higa MG, Zhao H, Vence L, Yadav SS, et al. Comparison of immune infiltrates in melanoma and pancreatic cancer highlights VISTA as a potential target in pancreatic cancer. Proceedings of the National Academy of Sciences. 2019; 116: 1692–1697. https://doi.org/10.1073/pnas.1811067116 PMID: 30635425

40. Connor AA, Gallinger S. Pancreatic cancer evolution and heterogeneity: integrating omics and clinical data. Nat Rev Cancer. 2022; 22: 131–142. https://doi.org/10.1038/s41568-021-00418-1 PMID: 34789870

41. Raghavan S, Winter PS, Navia AW, Williams HL, DenAdel A, Lowder KE, et al. Microenvironment drives cell state, plasticity, and drug response in pancreatic cancer. Cell. 2021; 184: 6119–6137.e26. https://doi.org/10.1016/j.cell.2021.11.017 PMID: 34890551

42. Herremans KM, Underwood PW, Riner AN, Neal DW, Tushoski-Alemán GW, Forsmark CE, et al. A protein-based machine learning approach to the identification of inflammatory subtypes in pancreatic ductal adenocarcinoma. Pancreatology. 2023; 23: 615–621. https://doi.org/10.1016/j.pan.2023.06.007 PMID: 37391359

43. Lippitz BE. Cytokine patterns in patients with cancer: a systematic review. Lancet Oncol. 2013; 14: e218–e228. https://doi.org/10.1016/S1470-2045(12)70582-X PMID: 23639322

44. De Boeck A, Ahn BY, D'Mello C, Lun X, Menon S V., Alshehri MM, et al. Glioma-derived IL-33 orchestrates an inflammatory brain tumor microenvironment that accelerates glioma progression. Nat Commun. 2020; 11: 4997. https://doi.org/10.1038/s41467-020-18569-4 PMID: 33020472

45. Garcia Garcia CJ, Huang Y, Fuentes NR, Turner MC, Monberg ME, Lin D, et al. Stromal HIF2 Regulates Immune Suppression in the Pancreatic Cancer Microenvironment. Gastroenterology. 2022; 162: 2018–2031. https://doi.org/10.1053/j.gastro.2022.02.024 PMID: 35216965

46. Jiang H, Hegde S, Knolhoff BL, Zhu Y, Herndon JM, Meyer MA, et al. Targeting focal adhesion kinase renders pancreatic cancers responsive to checkpoint immunotherapy. Nat Med. 2016; 22: 851–860. https://doi.org/10.1038/nm.4123 PMID: 27376576

47. Sharbeen G, McCarroll JA, Akerman A, Kopecky C, Youkhana J, Kokkinos J, et al. Cancer-Associated Fibroblasts in Pancreatic Ductal Adenocarcinoma Determine Response to SLC7A11 Inhibition. Cancer Res. 2021; 81: 3461–3479. https://doi.org/10.1158/0008-5472.CAN-20-2496 PMID: 33980655

48. Hecht JR, Lonardi S, Bendell J, Sim H-W, Macarulla T, Lopez CD, et al. Randomized Phase III Study of FOLFOX Alone or With Pegilodecakin as Second-Line Therapy in Patients With Metastatic Pancreatic Cancer That Progressed After Gemcitabine (SEQUOIA). Journal of Clinical Oncology. 2021; 39: 1108–1118. https://doi.org/10.1200/JCO.20.02232 PMID: 33555926